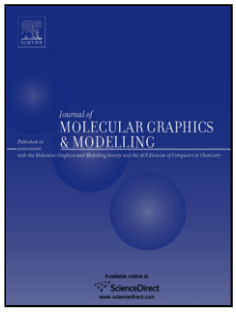

Title: How the cation-cation π-π stacking occurs: A theoretical investigation into ionic clusters of imidazolium

Author: Wei Gao Yong Tian Xiaopeng Xuan

PII: S1093-3263(15)00068-6
DOI: http://dx.doi.org/doi:10.1016/j.jmgm.2015.04.002
Reference: JMG 6530

To appear in: *Journal of Molecular Graphics and Modelling*

Received date: 29-11-2014
Revised date: 29-3-2015
Accepted date: 3-4-2015

Please cite this article as: W. Gao, Y. Tian, X. Xuan, How the cation-cation *rmpi-rmpi* stacking occurs: A theoretical investigation into ionic clusters of imidazolium, *Journal of Molecular Graphics and Modelling* (2015), http://dx.doi.org/10.1016/j.jmgm.2015.04.002

Graphic Abstract

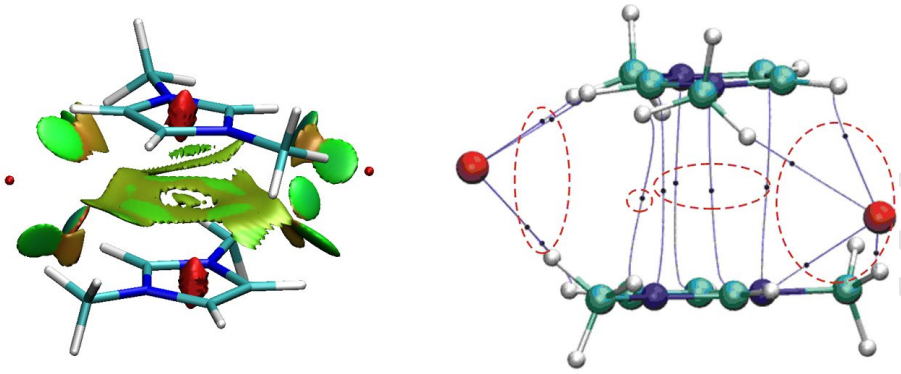

Reduced Density Gradient isosurface map (left) and Atom In Molecule (right) of the intermolecular interactions in the [Br][DMIM]···[DMIM][Br] dimers

Highlights

1) The nature of non-covalent interaction between cation-cation π-π stacking is explored theoretically.

2) Such interaction is different to common π-π interaction.

3) The occurrence of the interactions is attributed to a few contacts of C−H and halide.

How the cation-cation π-π stacking occurs: A theoretical investigation into ionic clusters of imidazolium

Wei Gao [a], Yong Tian [a,*], Xiaopeng Xuan[b,*]

[a] School of Pharmacy, Guangdong Pharmaceutical University, Guangzhou, 510006, China

[b] Collaborative Innovation Center of Henan Province for Green Manufacturing of Fine Chemicals, Key Laboratory of Green Chemical Media and Reactions, Ministry of Education, School of Chemistry and Chemical Engineering, Henan Normal University, Xinxiang, Henan 453007, China

Abstract:

The cation-cation π-π stacking is uncommon but it is essential for the understanding of some supramolecular structures. We explore theoretically the nature of non-covalent interaction occurring in the stacked structure within modeled clusters of 1,3-dimethylimidazolium and halide. The evidences of the Energy Decomposition Analysis (EDA) and Reduced Density Gradient (RDG) approach are different from those of common π-π interaction. Isosurfaces with RDG also illustrate the strength of the titled π-π interaction and their region. Additionally, we find that the occurrence of this interaction is attributed to a few C−H···X interactions, as depicted using Atom in Molecule (AIM) method. This work presents a clear picture of the typical cation-cation π-π interaction and can serve to advance the understanding of this uncommon interaction.

Keywords:
cation-cation π-π interaction, ionic liquids, clusters of imidazolium and halide

---

Corresponding Author:

*Y. Tian: e-mail, tian_yong_tian@163.com; Tel, 86-20-39352141.

*X. Xuan: e-mail, xpxuan@henannu.edu.cn; Tel, 83-373-3326335.

1. Introduction

Aromatic cations such as imidazolium, pyridinium and their derivatives have positive charge distributed in their rings, and are often used to synthesize functional materials, drug intermediates, organic crystals and ionic liquids (ILs) [1]. In the field of ILs particularly, imidazolium and its derivatives are well-known as the cationic components [2-3]. One major feature of these aromatic compounds is their ability to form π-π stacked structures. As an unusual structure, the cation-cation π-π stacking with imidazolium has been observed in ILs and is believed to play an important role in the structures [4-18]. As early as in 1993, X-ray crystallography of the 1-methylimidazolium salts revealed that cation-cation π-π stacking was possible [5]. Later, the short distances between aromatic-ring protons, as observed by NMR, have indicated the possible presence of close packing ring in imidazolium-based of neat ILs [6]. Meanwhile, some kinds of short-range cation-cation contacts were found by Molecular Dynamics (MD) method, among which the stacking was significant between neighboring imidazolium rings in these neat ILs [7-9]. Also, *ab intio* calculations suggested that cation-cation π-π stacked structures could be formed between two 1, 2, 4-triazolium cations in small clusters [10]. Recently, a statistical analysis of Cambridge Structural Database (CSD) [11] and high

level *ab initio* calculations [11-13] have shown that various structures of dimers of 1,3-dimethylimidazolium have been found and the complex interplay exhibited of structural features of hydrogen bond and π-π interactions in the presence of counter anions chloride/ bromide [11-13]. Either short or long alkyl chains connected to imidazolium cation, π-π stacking of the cation dimers have also been found between same charge ions in the crystalline [14-18].

A few theoretical works have been devoted to investigating some uncommon cation-cation π-π stacking, however, most of these studies are focused on its multiple structures and energies [4,11-15]. The counter anions like chloride or bromide have been a key to establishment of the cation-cation π-π stacking, but little is known about their association. In contrast to this uncommon π-π stacking, benzene dimer with face to face orientation is the prototypical system for studying common π-π stacking. And for the latter, although there is still considerable controversy in what forces are responsible, it is generally agreed that dispersion force [19-26] plays a major role. Obviously, it is more complicated to comprehend the π-π interactions between the two repulsive cation aromatic rings [27]. The nature of such unusual π-π stacking still remains largely unknown, either by atomic resolution experiments or theoretical investigations.

In this paper, we present an attempt to look into this case theoretically based on clusters of imidazolium, which are well-known as

the cationic components of ILs. We provide insights into the nature of cation-cation π-π interactions and moreover, to explain the formation mechanism of such interactions. Due to complications arising from environmental effects and competitive (or cooperative) non-covalent interactions, these results can not be directly revealed by instrumental approaches.

2. Methods of calculations

As an example for imidazolium-based ILs, we chose 1,3-dimethylimidazolium halide ([DMIM] [X]，X= F, Cl，Br and I). The initial structure of dimeric [DMIM][X], namely [X][DMIM]···[DMIM][X], was extracted from Ref [5] and the original anions were replaced by halogen anions [X]. The geometric optimization of [X][DMIM]···[DMIM][X] was carried out at the B3LYP-D3 [28] /maug-cc-pVTZ level. The B3LYP-D3 method is B3LYP with an empirical dispersion correction (Grimme's third version) [29] while the basis set maug-cc-pVTZ [30] is to use minimally augmentation (maug-) instead of full augmentation (aug-) [31-32]. This approach is an ideal balance between speed and accuracy for non-covalent interactions by theoretical calculations. Pseudopotentials (PP) [33-34] were used for Br and I atoms with maug-cc-pVXZ-PP basis set in order to consider the relativistic effects. Interacting energy were calculated by Gaussian 09

(version D01) [35], following B3LYP-D3, M06-2X and MP2 methods with aug-cc-pVTZ or aug-cc-pVTZ-PP basis sets. Additionally, we decomposed interacting energies into the energetic components using the new energy decomposition analysis GKS-EDA scheme [36], which is developed from the approach of generalized Kohn-Sham (GKS) and localized molecular orbital energy decomposition analysis (LMO-EDA) [37] methods. The GKS-EDA calculation was performed at the same level as the geometric optimization, with modified version of GAMESS 2012 [38] codes. Besides GKS-EDA, the interacting energies were counterpoise-corrected with the technique of Boys and Bernardi to avoid the basis set superposition errors (BSSE) [39]. Natural population analysis (NPA) [40] of the dimers were preformed at the MP2/aug-cc-pVTZ (aug-cc-pVTZ-PP) level, using the NBO version 3.1 [41] within the Gaussian 09 program. The wavefunction analysis using the wavefunction file in wfx format was produced with the same level to NBO analysis. The wavefunction analysis of Reduced Density Gradient (RDG) approach [42] and Atom In Molecule (AIM) [43] was calculated with Multiwfn 3.2 [44] and graphed with VMD 1.9.1 [45]. In addition, we compared the common π-π stacked structure (benzene dimer of face-to-face orientation) with the uncommon ones. The structure of benzene dimer was determined by a local minimum of potential energy surface (PES) (B3LYP-D3/ maug-cc-pVXZ) by way of varying the equilibrium intermolecular

separation for each monomer. Such an approach has been widely used [20-26].

3. Results and Discussions

3.1 The geometries and interactions for cation-cation π-π stacking

Our optimized results show that the dimer [F][DMIM]···[DMIM][F] could not reach the π-π stacked geometry and therefore, the discussion involved F anions is excluded from this study.

The other three optimized structures of dimers ([X][DMIM]···[DMIM][X], X=Cl, Br and I) are illustrated in Fig. 1, and the corresponding parameters for quantitative configurations are given in Fig. S1 and Table S1. All three optimized dimers show similar cage-like configurations, consisted of two [DMIM] units linked by [X]. The two [DMIM] ring planes are nearly face-to-face orientations with each other and the distances between their centers of ring vary from 3.6 to 3.7 Å (Fig. S1 and Table S1). All these three arrangements and their distances are in favor of the π-π interactions [20, 22, 26]. Similar structure has been found as the low energy conformer for the [Cl][DMIM]···[DMIM][Cl][12-13]. Meanwhile, The cage-like configurations also bring more distinct C−H···X interactions to be formed, which is supported by the fact that a number of H atom are in close proximity to halide. Three groups of C−H···X interactions can be identified. The first group C(2)−H···X comes from the halide and the ring protons located at C2 site (Fig. 2). Such

interaction is believed to play a prominent role [4,46] in imidazolium-based ILs. The second group C(4)−H···X is the halide and the ring protons located at C4 site while the third C−H(CH_3)···X is the halide and the methyl protons.

Several previous studies have indicated that the existence of anions is a key to the formation of stable cation-cation π-π stacked structure [4,10-13,27]. Different from the formation of common π-π stacking which includes only two benzene monomers, the formation of the titled π-π interaction requires the existence of the [X] anions besides two cation [DMIM] rings. Therefore, we treat each ions pair depending on the C(2)−H···X (primary interaction relative to the other ones) as a monomer (Fig. 3). Consequently, such π-π stacking can be regarded as one [DMIM][X] interacting with the other [DMIM][X]. In this way, the C(2)−H···X interaction is blocked when calculating the intermolecular energy between monomers. Under this consideration, the strength of non-covalent interactions between the two monomers follows the order [Cl][DMIM]···[DMIM][Cl]>[Br][DMIM]···[DMIM][Br]>[I][DMIM]···[DMIM][I] (Table 1). Obviously, these binding energies are much larger than that of common stacked π-π complex of a benzene dimer [20-26]. Such differences are at least partially attributable to the strong ions pair interactions like C−H(CH_3)···X and C(4)−H···X between the [DMIM] of one monomer and the [X] of the other one. Hunt and co-workers referred

to these C−H···X interactions between two anions and cations as the doubly ionic H-bond [4]. It has been recognized for some time that the hydrogen bond is important within the IL community [4, 46].

Quantitative insights into interacting energy come from the decomposition of interaction energy. The GKS-EDA scheme [36,47] is expressed by Eq. (1) and provides some clues to explore the nature of the binding energy.

$$\Delta E_{tot}=\Delta E_{ele}+\Delta E_{ex}+\Delta E_{rep}+\Delta E_{pol}+\Delta E_{corr}+\Delta E_{disp} \quad (1)$$

ΔE_{ele}, as the electrostatic interaction, can be obtained from monomers' Kohn-Sham(K-S) orbitals. ΔE_{rep} and ΔE_{ex} is the repulsion interaction and exchange interaction respectively, arising from the normalization and anti-symmetrization of K-S determinants. The $\Delta E_{rep}+\Delta E_{ex}$ can be regarded as repulsion effect. ΔE_{pol} is associated with the polarization interaction due to the variation on K-S orbitals by SCF process. ΔE_{corr} accounts for the correlation interaction defined as the difference of the GKS correlation energy from monomers to supermolecule. ΔE_{disp} is the dispersion interaction which is optional for dispersion correction DFT [36,47].

We use the same model of monomer to perform the GKS-EDA (Fig. 3). The total energy ΔE_{tot} and their energy components are reported in Table 2. Obviously, the stabilities and geometries of the dimers [X][DMIM]···[DMIM][X] depend upon the attractive and repulsive

interactions as well as their respective contributions, which are competitive with each other. On the one hand, the main attractive contributions come from electrostatics and polarization, mainly related to the formation of C−H···X interactions. The dispersion (ΔE_{disp}) energy terms are also evident, reaching ~10 kcal/mol. Furthermore, the dispersion energy $\Delta E_{disp(DMIM\text{-}DMIM)}$, occurring in two cation rings [DMIM]···[DMIM] by themselves without [X], are significant. And the percentages of $\Delta E_{disp(DMIM\text{-}DMIM)}$ to ΔE_{disp} is up to 55−63%. Clearly, it can be inferred that the majority of dispersion effect comes from the stacking of two cation rings. On the other hand, the repulsive contribution (ΔE_{rep} + ΔE_{ex}) provides a kind of background against the attractive contributions of electrostatics, polarization and dispersion. Therefore, the GKS-EDA results from the modeled dimers of 1,3-dimethylimidazolium and halide can explain the fact that the stability of dimers is dominated by electrostatic interaction but polarization and dispersion makes appreciable contributions.

In contrast to the [X][DMIM]···[DMIM][X], the benzene dimer with face-to-face orientation, is also studied at the same level. The distance between the two ring centers is 3.9 Å, which closely resembles those of high levels of theory (for example, CCSD(T)/CBS) [21-26]. Table 2 also lists the GKS-EDA result of benzene dimer. It is clear that in benzene dimer that the major contribution to the interaction energy arises from

dispersion, whereas the electrostatic and polarization contributions are negligibly weak. The results are in close agreement to Ref [20,22,24,26]. Likewise, the dispersion is largely cancelled by repulsion term. Obviously, the kind of cation-cation π-π interaction dominated by electrostatic contributions is different to common π-π interaction governed by dispersion.

3.2 The features of the cation-cation π-π interaction

To visualize and characterize the uncommon interaction, we present an approach of reduced density gradient (RDG) to map and analyze the interactions within [X][DMIM]···[DMIM][X] complexes. This approach, proposed by Yang's group, depends on RDG isosurfaces at low electron density values [42]. The RDG approach can qualitatively describe not only the nature and strength of non-covalent interaction but also their interaction region and characters [42, 48].

The C−H···X and π-π types of non-covalent interactions are visualized in the plots of the RDG domains from Fig. 4. Some RDG isosurfaces, distributed between [DMIM] and [X], is displayed as small disk-shaped with yellow or green. We easily recognize these attractive non-covalent regions midway between contact atoms X and H as C−H···X interactions. The RDG isosurfaces with yellow or green colors indicate that such interactions are not strong.

Undoubtedly, the area involving π-π interactions is worthy of more

attention. For each [X][DMIM]···[DMIM][X], there is one broad disk-shaped RDG domain (concave surfaces with holes, shown in green) in the region between the two cation rings. These RDG isosurfaces of broad disk-shaped are obviously derived from the interaction of two extended π electronic clouds unique to [DMIM]. The color code of green stands for weak attractions, which can be attributed to Van der Waals' force contribution. Clearly, these Van der Waals' interactions represent the important contributions to the stability of this dimer unit, as predicted by the GKS-EDA method. Meanwhile, a strong steric effect (shuttle-shaped, shown in red) is simultaneously shown in the regions of the center of the rings. It originates from the fact that each atom in a rigid aromatic ring occupies a certain amount of space, leading to the steric repulsive effect [42, 48]. The RDG domains distributed between the cation-cation stacked rings (Fig. 4) are similar to those between the two benzenes stacked rings (both of them have broad disk-shaped and red shuttle-shaped) (Fig. 5 (a)). However, anions [X] are the indispensable part of formation of the titled cation-cation π-π stacking therefore, the anions and cations should be regarded as an integration rather than separation. While some of the fundamental features of the RDG domains between the cation-cation stacked rings remain similar to those between the two benzenes stacked rings, there are a few unique qualities due to the C−H···X interactions of varying position and strength (correspond to the RDG domains between

atom H and X). Thus, these cation-cation π-π interactions can not be considered as the common π-π interaction based on the RDG picture and the GKS-EDA results. The picture and energy resulted from different type of π-π stacking need to be carefully explored and to ensure all the weak interactions are recovered.

3.3 The origins for the stability of cation-cation π-π interaction

The [DMIM] with the positive charge is distributed on the aromatic ring. As for [X][DMIM]···[DMIM][X], the net NPA charge distributed on each [DMIM] ring except for the two $-CH_3$ substituents has a steady positive charge with the values being +0.281e, +0.276e and +0.271e, respectively (Fig. 1). Obviously, this leads to a repulsion between two cation [DMIM] and definitely has an unfavorable effect on π-π stacking. Furthermore, the distance between the two [DMIM] rings in all three dimers (3.6 Å ~3.7 Å) is shorter than that between rings in the benzene dimer (3.90 Å). Considering the short distance, how can π-π interactions are established between two repulsive cations? The answer is of course related to the strong electrostatic attraction of the cation [DMIM] rings and anion [X], but its role is less clear. Further information is still necessary. The AIM method [43] gives another approach to clarify this issue. The molecular topological structure can be determined by the positions of critical points (CPs) including bond critical points (BCP), ring critical points (RCP) and cage critical points (CCP), as well as their

bond paths (BP) connecting these CPs [43]. Among these CPs, the BCPs is especially important as they are able to depict which atoms belong to each interaction, and their strength can be measured quantitatively by electronic density ρ(r) at BCPs [43,49].

The topological molecular graphs [X][DMIM]···[DMIM][X] of BCPs and their BPs are shown in Fig. 6, along with their data (electron density ρ(r) and its Laplacian of electron density $\nabla^2\rho(r)$) presented in Table 3. In these cases, all CPs satisfy the Poincare' Hopf relationship [43]. These graphs concerning BCPs and BPs are remarkably similar features, and all the BCPs can be divided into three cases: C−H···X, π-π and −C−H···H−C− interaction. In the first case, the attractive contacts C−H···X can be distinguished from each other. The atom H comes from $-CH_3$ substituents, C(2)−H and C(4)−H on the ring sketch, respectively (Fig. 2). In these dimer, The C(2)−H···X interactions identified as weak hydrogen bond are stronger [11,46,50] than those of C−H(CH_3)···X or C(4)−H···X interactions, measured by the average of the electronic density (Table 3). π-π interaction as second case, a few BCPs and their BPs connecting the atoms pair of C···C, C···N or N···N clearly characterize the existence of non-covalent interactions between the two [DMIM] rings during two cations stacking. Similar topographical features appear in common stacked π-π dimers [49] and the benzene dimer (Fig. 5 (b)).

Moreover, by AIM analysis, we can explain why the cation aromatic contacts can create π-π stacking. It can be ascribed to a few C−H···X contacts between the X and H atoms. Each attraction of these contacts is not strong, according to its magnitude of the average ρ(r) from 0.0114 to 0.0262 a.u. However, the total of these weak contacts is strong enough (ranging from 0.111 to 0.141 a.u.), owing to their number of up to 8 in each dimer (Fig. 6). The resultant of a few C−H···X interactions provides a driving force to enforce the two cation [DMIM] rings to be close and to adopt the parallel conformation. In other words, the two cations, with the help of C−H···X forces, can induce the uncommon π-π interaction when their arrangement and distance meet the π-π stacking. Instead of relying on implicit information from experimental observations [5-6,16,50], These AIM findings demonstrate that the C−H···X contacts play an important role in establishing cation-cation stacking.

It is necessary to note that such a conclusion is limited to the simple symmetric ions of [DMIM] and [X]. Extrapolating these findings from the present system to other complex system can be risky. Evidently, the structural complexity and flexibility of ILs increase when simple [X] anions are replaced by complex anions like PF_6 or cations with methyl group are changed to those with long alkyl chain. As a result, the π-π stacking as an orderly assemblage and its behavior suggested in this paper may be changed accordingly by their complexity and flexibility.

Therefore, very careful examination is required to extend the decision to complex anions or cations.

At last，interestingly, the BCPs also appear between two $-CH_3$ subsistents of different rings (Fig. 6) and can be classified as −C−H···H−C− interaction. Due to the limitation of AIM theory [51], the presence of the BCPs is questionable. The distances between the two corresponding H atoms are 2.76, 2.85 and 2.92 Å in these three cases, respectively; all of them are larger than the sum of their van der Waals radii (2.4 Å). Therefore, the strength of −C−H···H−C− interactions, if it really existed, might be very weak and could even be neglected.

4. Conclusions

In this paper, the cation-cation π-π stacked structures in clusters of the two imidazolium cations and two halogen anions [X][DMIM]···[DMIM][X] are optimized and analyzed. The results from EDA show that the stabilization of clusters is dominated by electrostatic interaction but polarization and dispersion make appreciable contributions. RDG isosurfaces depict the characteristics of the non-covalent interaction of cation-cation π-π stacked structure, which are similar to the common π-π interaction but have different features. The evidences of the EDA and RDG approach are different from those of common π-π interaction observed in benzene dimer. Moreover, we demonstrate that the occurrence of a few C−H···X contacts is the key to

the cation-cation π-π interactions by AIM analysis. These results give a deeper insight into cation-cation π-π interactions and provide a clear picture of the interactions theoretically. However, extreme care should be taken in applying these conclusions to other ILs because such stacking is very system-dependent.

Acknowledgements

This work is supported by the Natural Science Foundation of China (Nos. 21173069, 21373061), the Natural Science Foundation of Guangdong Province, China (No. S2013040013904) and the Medical Science Foundation of Guangdong Province, China (No. 2015120134413281). The Authors also acknowledge the support of The Research Foundation for Young Teachers of School of Pharmacy, Guangdong Pharmaceutical University.

References

[1] N. Noujeim, L. Leclercq, A. R. Schmitzer, Imidazolium Cations in Organic Chemistry: From Chemzymes to Supramolecular Building Blocs. Curr. Org. Chem. 14 (2010) 1500–1516.

[2] R.Sharma, R. K.Mahajan, Influence of various additives on the physicochemical properties of imidazolium based ionic liquids: a comprehensive review. RSC Adv. 4 (2014) 748–774.

[3] J. Dupont, From Molten Salts to Ionic Liquids: A “Nano” Journey. Acc. Chem. Res. 44 (2011) 1223–1231.

[4]P. A. Hunt, C. R. Ashworth, R. P. Matthews, Hydrogen bonding in ionic liquids. Chem. Soc. Rev., 44 (2015) 1257-1288

[5] J. S. Wilkes, M. J. Zaworotko, Manifestations of noncovalent interactions in the solid state. Dimeric and polymeric self-assembly in imidazolium salts via face-to-face cation-cation π-stacking. Supramol. Chem. 1 (1993) 191–193.

[6] A. Mele, G. Roman, M. Giannone, E. Ragg, G. Fronza, G. Raos, V. Marcon, The Local Structure of Ionic Liquids: Cation–Cation NOE Interactions and Internuclear Distances in Neat [BMIM][BF_4] and [BDMIM]-[BF_4]. Angew. Chem. Int. Ed. 45 (2006) 1123–1126.

[7] B. L. Bhargava, S. Balasubramanian, Intermolecular structure and dynamics in an ionic liquid: A Car–Parrinello molecular dynamics simulation study of 1,3-dimethylimidazolium chloride. Chem. Phys. Lett. 417 (2006) 486–491.

[8] N. M. Micaelo, A. M. Baptista, C. M.Soares, Parameterization of 1-Butyl-3-methylimidazolium Hexafluorophosphate/Nitrate Ionic Liquid for the GROMOS Force Field. J. Phys. Chem. B 110 (2006) 14444–14451.
[9] B. Qiao, C. Krekeler, R. Berger, L. D. Site, C. Holm, Effect of Anions on Static Orientational Correlations, Hydrogen Bonds, and Dynamics in Ionic Liquids: A Simulational Study. J. Phys. Chem. B 112 (2008) 1743–1751.
[10] H. Li, J. A. Boatz, M. S. Gordon, Cation-Cation π-π Stacking in Small Ionic Clusters of 1,2,4-Triazolium. J. Am. Chem. Soc. 130 (2008) 392–393.
[11] I. Geronimo, N. J. Singh, K. S. Kim, Nature of anion-templated π+ - π+ interactions. Phys. Chem. Chem. Phys. 13 (2011) 11841–11845.
[12] R. P. Matthews, T. Welton, P. A. Hunt, Competitive pi interactions and hydrogen bonding within imidazolium ionic liquids. Phys. Chem. Chem. Phys. 16 (2014) 3238–3253.
[13] R. P Matthews, C. Ashworth, T. Welton, P. A Hunt, The impact of anion electronic structure:similarities and differences in imidazolium based ionic liquids. J. Phys.-Condens. Mat. 26 (2014) 284112
[14] J. Kohanoff, C. Pinilla, T. G. A. Youngs, E. Artacho, J. M. Soler, Dispersion interactions in room-temperature ionic liquids: Results from a non-empirical density functional. J. Chem. Phys. 135 (2011) 154505.
[15] M. G. Del Pópolo, C. Pinilla, P. Ballone, Local and semilocal density functional computations for crystals of 1-alkyl-3-methylimidazolium salts. J. Chem. Phys. 126 (2007) 144705
[16] G. Laus, G. Bentivoglio, V. Kahlenberg, K. Wurst, G. Nauer, H. Schottenberger, M. Tanaka, H.-U. Siehl, Conformational Flexibility and Cation−Anion Interactions in 1-Butyl-2,3-dimethylimidazolium Salts. Cryst. Growth Des. 12 (2012) 1838−1846.
[17] J. D. Holbrey, W. M. Reichert, I. Tkatchenko, E. Bouajila, O. Walter, I. Tommasid, R. D. Rogers, 1,3-Dimethylimidazolium-2-carboxylate: the unexpected synthesis of an ionic liquid precursor and carbene-CO_2 adduct. Chem. Commun.(2003) 28–29.
[18] N. J. Bridges, C. C. Hines, M. Smiglak, R. D. Rogers, An Intermediate for the Clean Synthesis of Ionic Liquids:Isolation and Crystal Structure of 1,3-Dimethylimidazolium Hydrogen Carbonate Monohydrate. Chem. Eur. J. 13 (2007) 5207–5212.
[19] C. R. Martinez, B. L.Iverson, Rethinking the term ‘‘pi-stacking’’. Chem. Sci. 3 (2012) 2191–2201.
[20] C. D. Sherrill, Energy Component Analysis of π Interactions. Acc. Chem. Res. 46 (2013) 1020–1028.
[21] T. Sato, T.Tsuneda, K.Hirao, A density-functional study on π -aromatic interaction: Benzene dimer and naphthalene dimer. J. Chem. Phys. 123 (2005) 104307.
[22] E .C. Lee, D. Kim, P. Jurečka, P. Tarakeshwar, P. Hobza, K.S. Kim, Understanding of Assembly Phemona by Aromatic-Aromatic Interactions: Benzene Dimer and the Substituted Systems. J. Phys. Chem. A 111 (2007) 3446–3457.
[23] C. D. Sherrill, T. Takatani, E. G. Hohenstein, An Assessment of Theoretical

Methods for Nonbonded Interactions: Comparison to Complete Basis Set Limit Coupled-Cluster Potential Energy Curves for the Benzene Dimer, the Methane Dimer, Benzene-Methane, and Benzene-H2S. J. Phys. Chem. A 113 (2009) 10146-10159.

[24] A. L. Ringer, C. D. Sherrill, Substituent Effects in Sandwich Configurations of Multiply Substituted Benzene Dimers Are Not Solely Governed By Electrostatic Control. J. Am. Chem. Soc. 131 (2009) 4574-4575

[25] S. E. Wheeler. Understanding Substituent Effects in Noncovalent Interactions Involving Aromatic Rings. Acc. Chem. Res. 46 (2013) 1029−1038.

[26] R. M. Parrish, C. D. Sherrill, Quantum-Mechanical Evaluation of π-π Versus Substituent-π Interactions in π Stacking: Direct Evidence for the Wheeler-Houk Picture. J. Am. Chem. Soc. 136 (2014) 17386-17389.

[27] S. Grimme, J.-P. Djukic, Cation-Cation "Attraction": When London Dispersion Attraction Wins over Coulomb Repulsion. Inorg. Chem. 50 (2011) 2619–2628.

[28] S.Zahn, D. R. MacFarlane, E. I. Izgorodina, Assessment of Kohn–Sham density functional theory and Møller–Plesset perturbation theory for ionic liquids. Phys. Chem. Chem. Phys. 15 (2013) 13664–13675.

[29] S. Grimme, J. Antony, S. Ehrlich, H. Krieg, A consistent and accurate ab initio parametrization of density functional dispersion correction (DFT-D) for the 94 elements H-Pu. J. Chem. Phys. 132 (2010) 154104.

[30] E. Papajak, J. Zheng, X. Xu, H. R. Leverentz, D.G. Truhlar, Perspectives on Basis Sets Beautiful: Seasonal Plantings of Diffuse Basis Functions. J. Chem. Theory Comput. 7 (2011) 3027–3034.

[31] A. D. McLean, G. S.Chandler, Contracted Gaussian basis sets for molecular calculations. I. Second row atoms, Z=11–18. J. Chem. Phys. 72 (1980) 5639.

[32] L. A. Curtiss, M. P. McGrath, J-P. Blaudeau, N. E. Davis, R. C. Binning, Jr., L. Radom, Extension of Gaussian2 theory to molecules containing third-row atoms Ga–Kr. J. Chem. Phys. 103 (1995) 6104.

[33] K.A. Peterson, D.Figgen, E.Goll, H. Stoll, M.Dolg, Systematically convergent basis sets with relativistic pseudopotentials. II. Small-core pseudopotentials and correlation consistent basis sets for the post-d group 16-18 elements. J. Chem. Phys. 119 (2003) 11113.

[34] K.A. Peterson, B. C. Shepler, D. Figgen, H. Stoll, On the spectroscopic and thermochemical properties of ClO, BrO, IO, and their anions. J. Phys. Chem. A 110 (2006) 13877−13883

[35] M. J. Frisch, G. W. Trucks, H. B. Schlegel, G. E. Scuseria, M. A. Robb, J. R. Cheeseman, G. Scalmani, V. Barone, B. Mennucci, G. A. Petersson, H. Nakatsuji, M. Caricato, X. Li, H. P. Hratchian, A. F. Izmaylov, J. Bloino, G. Zheng, J. L. Sonnenberg, M. Hada, M. Ehara, K. Toyota, R. Fukuda, J. Hasegawa, M. Ishida, T. Nakajima, Y. Honda, O. Kitao, H. Nakai, T. Vreven, J. A. Montgomery, Jr., J. E. Peralta, F. Ogliaro, M. Bearpark, J. J. Heyd, E. Brothers, K. N. Kudin, V. N. Staroverov, R. Kobayashi, J. Normand, K. Raghavachari, A. Rendell, J. C. Burant, S. S. Iyengar, J. Tomasi, M. Cossi, N. Rega, J. M. Millam, M. Klene, J. E. Knox, J. B. Cross, V. Bakken, C. Adamo, J. Jaramillo, R. Gomperts, R. E. Stratmann, O. Yazyev, A. J. Austin, R. Cammi, C. Pomelli, J. W. Ochterski, R. L. Martin, K. Morokuma, V.

G. Zakrzewski, G. A. Voth, P. Salvador, J. J. Dannenberg, S. Dapprich, A. D. Daniels, Ö. Farkas, J. B. Foresman, J. V. Ortiz, J. Cioslowski, D. J. Fox, Gaussian 09, Revision D.01, Gaussian Inc., Wallingford, CT, 2013.

[36] P. Su, Z. Jiang, Z. Chen, W. Wu, Energy Decomposition Scheme Based on the Generalized Kohn–Sham Scheme. J. Phys. Chem. A 118 (2014) 2531−2542.

[37] P. Su, H. Li, Energy decomposition analysis of covalent bonds and intermolecular Interactions. J. Chem. Phys. 131 (2009) 014102.

[38] M. S. Gordon, M. W. Schmidt, in: C. E.Dykstra, G.Frenking, K. S. Kim,G. E. Scuseria (Eds.), Theory and applications of computational chemistry, Elsevier, Amsterdam, 2005, pp.1167–1189.

[39] S. F. Boys, F. Bernardi, The Calculation of Small Molecular Interactions by the Differences of Separate Total Energies. Some Procedures with Reduced Errors. Mol. Phys. 19 (1970) 553−566.

[40] E. D. Glendening, C. R. Landis, F. Weinhold, Natural bond orbital methods. WIREs Comput. Mol. Sci. 2 (2012) 1–42.

[41] E. D. Glendening, A. E. Reed, J. E. Carpenter, F. Weinhold, NBO Version 3.1.

[42] E. R. Johnson, S. Keinan, P. Mori-Sánchez, J. Contreras-García, A. J. Cohen, W. Yang, Revealing Noncovalent Interactions. J. Am. Chem. Soc. 132 (2010) 6498–6506.

[43] J. Poater, M. Duran, M. Solà, B. Silvi, Theoretical Evaluation of Electron Delocalization in Aromatic Molecules by Means of Atoms in Molecules (AIM) and Electron Localization Function (ELF) Topological Approaches. Chem. Rev. 105 (2005) 3911–3947.

[44] T. Lu, F. Chen, Multiwfn: A multifunctional wavefunction analyzer. J. Comp. Chem. 33 (2012) 580–592.

[45] W. Humphrey, A. Dalke, K. Schulten, "VMD - Visual Molecular Dynamics". J. Mol. Graph. 14 (1996) 33–38.

[46] V. Kemptera, B.Kirchner, The role of hydrogen atoms in interactions involving imidazolium-based ionic liquids. J. Mol. Struct. 972 (2010) 22–34.

[47] X Chang, P Su, W Wu. Internal rotation barrier of the XH3-YH3(X, Y = C or Si) molecules.An energy decomposition analysis study. Chem Phys Lett 610–611 (2014) 246–250.

[48] G. Saleh, C. Gatti, L. Lo Presti, J. Contreras-García, Revealing Non-covalent Interactions in Molecular Crystals through Their Experimental Electron Densities. Chem. Eur. J. 18 (2012) 15523 –15536.

[49] I .S. Konovalova, Y.V. Nelyubina, K.A. Lyssenko, B.V. Paponov, O.V. Shishkin, Intra- and Intermolecular Interactions in the Crystals of 3,4-Diamino-1,2,4-triazole and Its 5-Methyl Derivative. Experimental and Theoretical Investigations of Charge Density Distribution. J. Phys. Chem. A 115 (2011) 8550–8562.

[50] T. Gutel, C. C. Santini, A.A.H. Pádua, B.Fenet, Y.Chauvin, J.N.C. Lopes, F. Bayard, M. F. C. Gomes, A. S. Pensado, Interaction between the π-System of Toluene and the Imidazolium Ring of Ionic Liquids: A Combined NMR and Molecular Simulation Study. J. Phys. Chem. B 113 (2009) 170–177.

[51] J. R. Lane, J. Contreras-García, J.-P. Piquemal, B. J. Miller, H. G. Kjaergaard,

Are Bond Critical Points Really Critical for Hydrogen Bonding? J. Chem. Theory Comput. 9 (2013) 3263−3266.

Figures

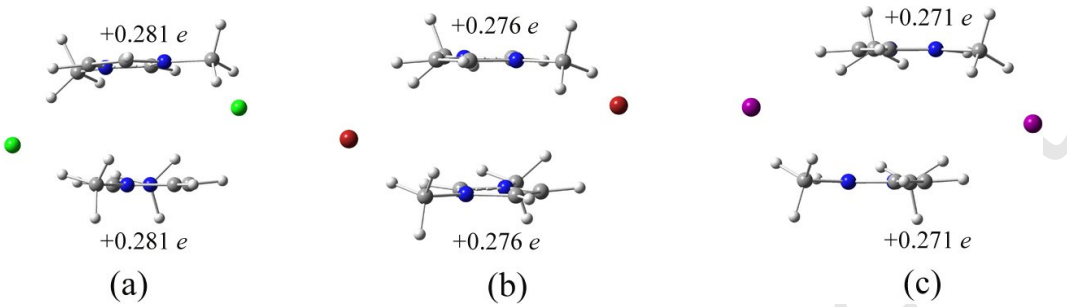

Fig. 1. Three optimized structures of the clusters [X][DMIM]···[DMIM][X] (X=Cl (a), Br (b), I (c)). The net NPA charges on [DMIM] rings except for the two $-CH_3$ groups are also provided.

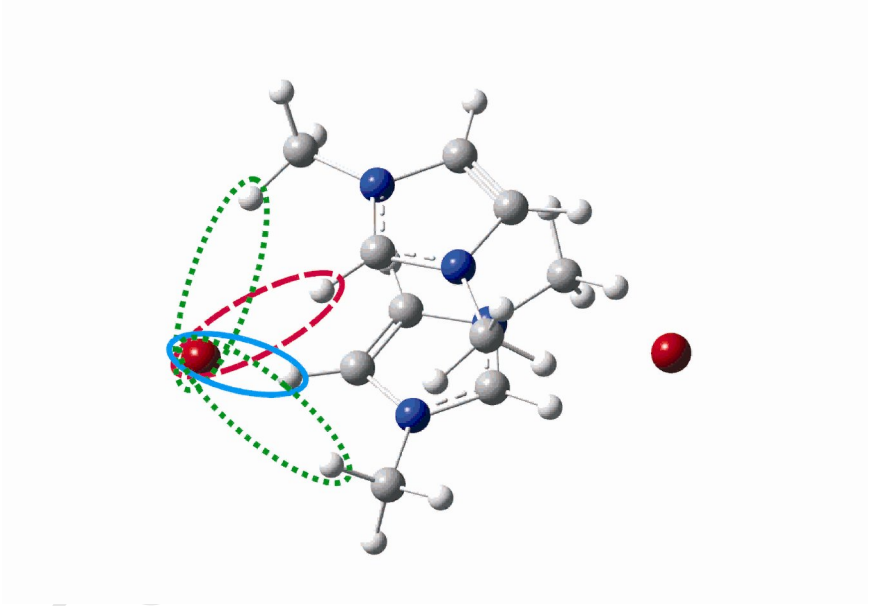

Fig. 2. The diagram of three classes of $C(CH_3)-H\cdots X$, $C(2)-H\cdots X$ and $C(4)-H\cdots X$. The similar interacting mode on the right is not showed.

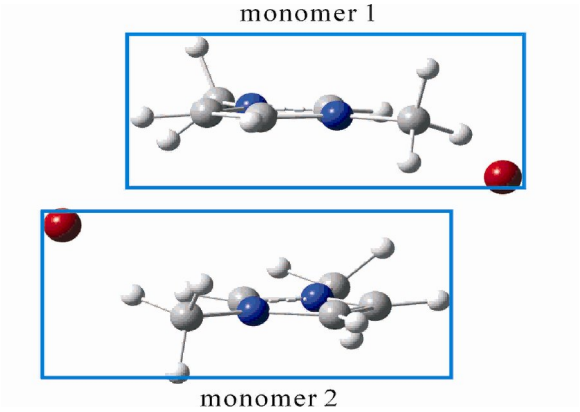

Fig. 3. The illustration of the monomer in dimer [X][DMIM]···[DMIM][X]

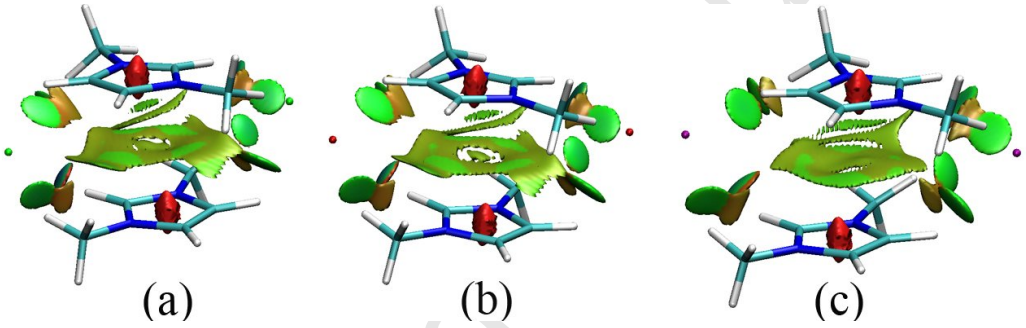

Fig. 4. Reduced density gradient (RDG) isosurface map of an intermolecular interaction in the [X][DMIM]···[DMIM][X] (X= Cl (a), Br (b) , I (c)) dimers, associated with the surfaces corresponding to s = 0.5 au and the isosurfaces far away from the interacting areas are screened out for clarity.

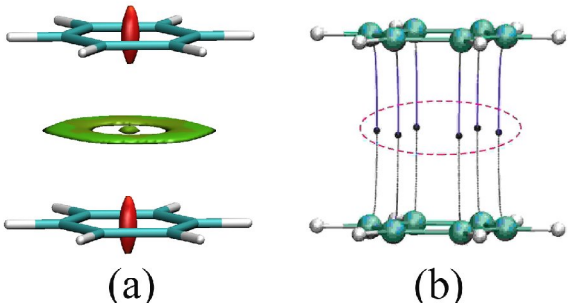

Fig. 5. Reduced density gradient (RDG) isosurface map (a) and Atom in Molecules (AIM) molecular graphs (b) of an intermolecular interaction for benzene dimer. The distance between the two ring centers is 3.9 Å.

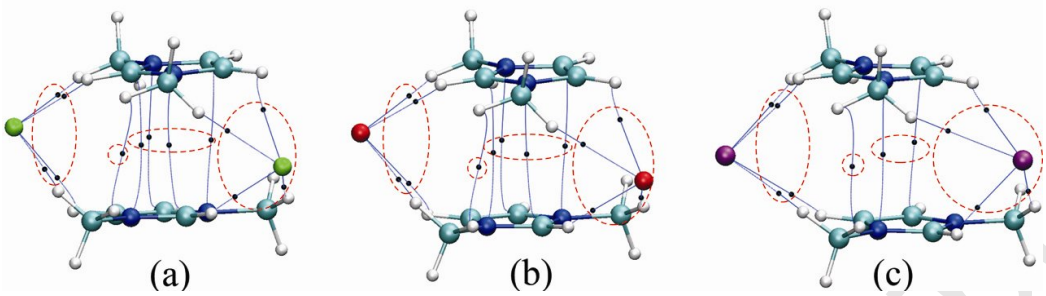

Fig. 6. The molecular graphs for the structures of [X][DMIM]···[DMIM][X] (X= Cl (a), Br (b) , I (c)) dimers obtained using AIM analysis. Small blue spheres and blue line represent BCP and BP, respectively. The BCPs in dotted circles are attributed to C−H···X, −C−H···H−C−, π-π and C−H···X interactions, respectively. The RCP and CCP are not displayed.

Tables

Table 1. BSSE corrected interaction energies (kcal/mol) of investigated structures of the [X][DMIM]···[DMIM][X] (X=Cl, Br, I) dimers calculated at various levels of theory

Methods	[X]=Cl	[X]=Br	[X]=I
B3LYP-D3	-34.21	-32.66	-30.38
M06-2X	-34.53	-32.31	-29.85
MP2	-36.73	-35.03	-32.28

Table 2. The results of GKS-EDA decomposition of the interaction energies (kcal/mol) of [X][DMIM]···[DMIM][X] (X=Cl, Br, I) dimers at the B3LYP-D3/maug-cc-pVTZ and B3LYP-D3/maug-cc-pVTZ-PP level of theory.

	[X]=Cl	[X]=Br	[X]=I	Benzene dimer[c]
ΔE_{tot} [a]	-33.66	-32.12	-29.27	-1.49
ΔE_{ele}	-38.8	-37	-34.19	-0.09
ΔE_{ex}	-57.41	-55.92	-52.58	-5.40
ΔE_{rep}	96.64	94.2	89.59	8.90
ΔE_{pol}	-17.78	-16.94	-17.45	0.06
ΔE_{corr}	-4.43	-4.45	-3.53	-0.87
ΔE_{disp}	-11.87	-12.02	-11.11	-4.09
$\Delta E_{disp(DMIM-DMIM)}$	-7.46	-7.03	-6.09	
net ΔE_{rep} [b]	39.23	38.28	37.01	3.50

[a] $\Delta E_{tot} = \Delta E_{ele}+\Delta E_{ex}+\Delta E_{rep}+\Delta E_{pol}+\Delta E_{corr}+\Delta E_{disp}$

[b] net $\Delta E_{rep} = \Delta E_{ex}+\Delta E_{rep}$

[c] The distance between the two ring centers is 3.9 Å.

Table 3. Electronic density ρ(r) (a.u.) and its Laplacian of electron density $\nabla^2\rho(r)$ (a.u.) for different C−H···X interactions and pi-pi stacking within the [X][DMIM]···[DMIM][X] (X=Cl, Br, I) dimers, shown in Fig. 6.

	C−H(CH_3)···X		C(4)−H···X		C(2)−H···X		π-π	
	ρ(r)	$\nabla^2\rho(r)$	ρ(r)	$\nabla^2\rho(r)$	ρ(r)	$\nabla^2\rho(r)$	ρ(r)	$\nabla^2\rho(r)$
[X]=Cl	0.0148	0.0421	0.0133	0.0413	0.0262	0.0683	0.00356	0.0116
	0.0148	0.0421	0.0133	0.0413	0.0262	0.0683	0.00356	0.0116
	0.0164	0.0468					0.00394	0.0136
	0.0164	0.0468					0.00394	0.0136
[X]=Br	0.0134	0.0337	0.0129	0.0354	0.0231	0.0546	0.00335	0.0107
	0.0134	0.0337	0.0129	0.0354	0.0231	0.0546	0.00335	0.0107
	0.0147	0.0369					0.00342	0.0118
	0.0147	0.0369					0.00342	0.0118
[X]=I	0.0114	0.0251	0.0136	0.0310	0.0182	0.0411	0.00266	0.0093
	0.0114	0.0251	0.0136	0.0310	0.0182	0.0411	0.00377	0.0106
	0.0123	0.0269						
	0.0123	0.0269						